Fabrication of Colloidal Stable, Thermosensitive, and Biocompatible Magnetite Nanoparticles and Study of Their Reversible Agglomeration in Aqueous Milieu

Munish Chanana,[†] Sabrina Jahn,[‡] Radostina Georgieva,[§] Jean-François Lutz,[||] Hans Bäumler,[§] and Dayang Wang*,[†]

Max Planck Institute of Colloids and Interfaces, 14424, Potsdam, Germany, Institute of Transfusion Medicine, Charité-Univeristätsmedizin Berlin, 10098, Berlin, Germany, Research group Nanotechnology for Life Science, Fraunhofer Institute for Applied Polymer Research, 14476, Potsdam, Germany, and Institute of Biotechnology, University of Cambridge, Tennis Court Road, Cambridge CB2 1QT, U.K.

Received January 15, 2009

A number of catechol-terminated copolymers of di(ethylene glycol) methyl ether methacrylate (MEO_2MA) and poly(ethylene glycol) methyl ether methacrylate (OEGMA) with varied MEO_2MA-to-OEGMA molar ratios were synthesized via atom transfer radical polymerization triggered by dopamine-derived initiators. They were grafted on magnetite nanoparticles (NPs) via ligand exchange, thus imparting the NPs with robust colloidal stability against salt and excellent biocompatibility. Of importance is that similar to the copolymers of MEO_2MA and OEGMA, their coated magnetic NPs showed a lower critical solution temperature. This leads to a reversible agglomeration of the resulting composite NPs in buffer and physiological solution in response to the environment temperature. This reversible and thermosensitive agglomeration were also observed within red blood cells after loading the resulting composite NPs into the cells. The agglomeration of magnetite NPs in red blood cells endowed the NP-loaded composite cells with a better magnetic response, for example, contrast enhancement for magnetic resonance imaging.

Introduction

For many practical applications it is necessary to switch nanoparticle (NP) agglomeration reversibly via external stimuli. As individual particles they are mobile and can easily cross small pores and interstices or be actively or passively transported,[1,2] for example, through the blood/brain barrier, whereas as agglomerates they are less mobile and may even clog pores. However, NP agglomerates may possess useful collective properties, for example, optical and electronic ones, and controlled release.[3−5] But controlled and reversible agglomeration represents a formidable challenge because typically, once agglomeration commences, NPs precipitate and attractive interactions between the particles remain dominant compared to thermal energy or repulsive interactions if they later are introduced by another stimulus. Here we present a solution to this problem and two practical applications, where magnetic NPs are coated by a thermoresponsive and biocompatible polymer, then introduced into an aqueous milieu or a cell where they can be reversibly agglomerated. These agglomerates exhibit a drastically increased magnetic response, which makes them amenable to manipulation by external magnetic field and useful for contrast enhancement in magnetic resonance imaging (MRI).

Table 1. Summary of Fe_3O_4@MEO_2MA_x-*co*-$OEGMA_y$ and Their LCSTs in Aqueous Media

		size (nm)			LCST (°C)	
samples	M_n of the polymer coating ($\times 10^4$)	polymer coated NPs	Fe_3O_4 cores	polymer shell thickness	H_2O	PBS
Fe_3O_4@OEGMA	4.2	22.8	6.4	8.2	95	76
Fe_3O_4@MEO_2MA_{70}-*co*-$OEGMA_{30}$	1.7	14.6	6.4	4.1	62	43
Fe_3O_4@MEO_2MA_{85}-*co*-$OEGMA_{25}$	2.1	21.8	9.1	6.4	42	39
Fe_3O_4@MEO_2MA_{90}-*co*-$OEGMA_{10}$	3.9	16.0	6.4	4.8	43	36
Fe_3O_4@MEO_2MA_{92}-*co*-$OEGMA_8$	3.4	16.0	6.4	4.8	36	33
Fe_3O_4@MEO_2MA	1.7	16.1	6.4	4.9	24	20

Fe_3O_4 NPs hold immense promise in biomedical applications such as drug targeting and MRI.[6−8] Currently they remain the only magnetic NPs that have been approved for clinical use because of their chemical stability, biocompatibility, and noncytotoxicity. Besides, they (including γ-Fe_2O_3 NPs) are rather easily synthesized via wet chemical methods, such as coprecipitation and thermal pyrolysis.[9] Nonetheless, their low saturation magnetization in an external magnetic

* To whom the correspondence should be addressed. E-mail: dayang.wang@mpikg.mpg.de. Fax: +49 331 5679202.
[†] Max Planck Institute of Colloids and Interfaces.
[‡] University of Cambridge.
[§] Charité-Univeristätsmedizin Berlin.
[||] Fraunhofer Institute for Applied Polymer Research.

(1) Alivisatos, A. P. *Sci. Am.* **2001**, *285*, 59–65.
(2) Medintz, I.; Uyeda, H.; Goldman, E.; Mattoussi, H. *Nat. Mater.* **2005**, *4*, 435–446.
(3) Colloir, C. P.; Vossmeyer, T.; Heath, J. R. *Annu. Rev. Phys. Chem.* **1998**, *49*, 371–404.
(4) Murray, C. B.; Kagan, C. R.; Bawendi, M. G. *Annu. Rev. Mater. Sci.* **2000**, *30*, 545–610.
(5) Weller, H. *Phil. Trans. R. Soc. London, Ser. A* **2003**, *361*, 229–240.
(6) Weissleder, R.; Bogdanov, A.; Neuwelt, E. A.; Papisov, M. *Adv. Drug Delivery Rev.* **1995**, *16*, 321–334.
(7) Lubbe, A. S.; Alexiou, C.; Bergemann, C. *J. Surg. Res.* **2001**, *95*, 200–206.
(8) Corot, C.; Robert, P.; Idee, J.-M.; Port, M. *Adv. Drug Delivery Rev.* **2006**, *58*, 1471–1504.

10.1021/cm900126r CCC: $40.75
Published on Web 04/13/2009

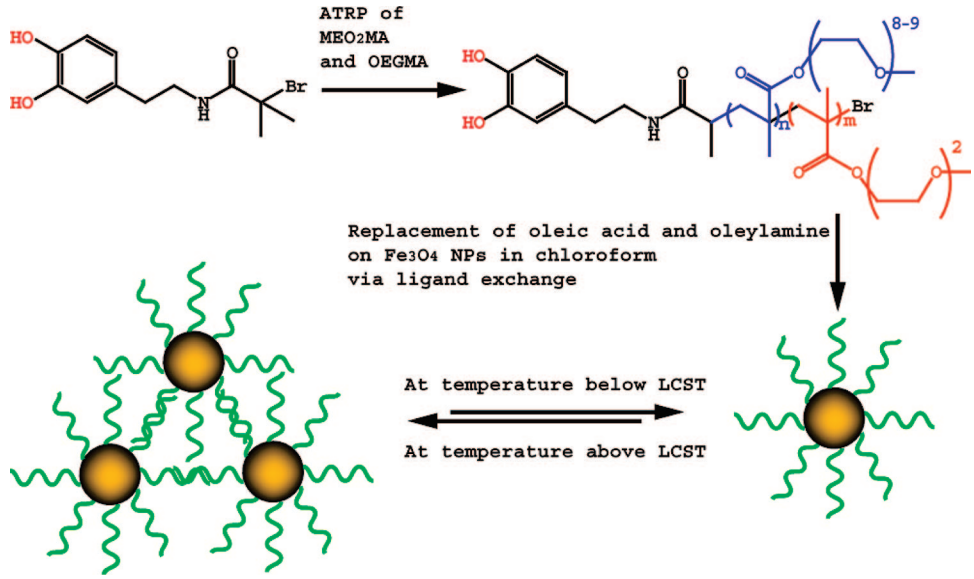

Figure 1. Schematic illustration of the grafting-to procedure of growth of MEO_2MA_x-*co*-$OEGMA_y$ brushes on Fe_3O_4 NPs and the temperature-sensitive agglomeration of the resulting NPs.

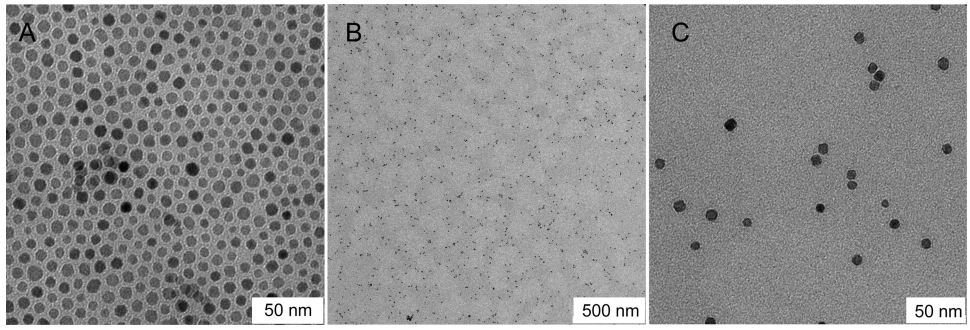

Figure 2. (A) TEM image of Fe_3O_4 NPs stabilized by oleic acid and oleylamine in chloroform. Low (B) and high (C) magnification TEM images of Fe_3O_4@MEO_2MA_{90}-*co*-$OEGMA_{10}$ NPs in water.

field largely limits the efficiency in a practical biomedical use, especially in vivo. To circumvent this challenge, four major strategies have been proposed: (1) optimization of the magnetic field design, (2) use of other materials with a larger magnetic moment, (3) increase of Fe_3O_4 NP sizes, and (4) Trojan-horse strategy—loading of Fe_3O_4 NPs into micrometer-sized carriers.[10] But each solution carries its own disadvantages correlated with circulation time and cyto-toxicity, for instance. Here we demonstrate a different way—using the environmental stimuli to reversibly switch Fe_3O_4 NP agglomeration—to improve their magnetic performance avoiding disadvantages as compared with the existing techniques. To tune agglomeration and disagglomeration of Fe_3O_4 NPs in a controlled manner, they were grafted with thermosensitive polymer brushes—random copolymers of 2-(2-methoxyethoxy) ethyl methacrylate (MEO_2MA) and oligo(ethylene glycol) methacrylate (OEGMA), with the aid of atom transfer radical polymerization (ATRP). The copolymers were marked as MEO_2MA_x-*co*-$OEGMA_y$, where x and y represent the molar fractions of MEO_2MA and OEGMA, respectively.

Recently a number of techniques have been developed to generate a highly hydrophilic polymer coating on NPs to improve the colloidal stability and impart them with multiple functionalities.[11−14] Among these techniques, ATRP is of great interest because it provides immense flexibility to incorporate various functional segments into one polymer chain and, most importantly, add one tailor-designed functional group to one end of the polymer chain.[15−17] We and other groups have recently anchored stimuli-sensitive polymer brushes on inorganic NPs via ATRP. However, the stimuli sensitivity of the polymer brushes grafted on NPs has been mainly used to control the interfacial behavior of

(9) Lu, A.; Salabas, E. L.; Schuth, F. *Angew. Chem., Int. Ed.* **2007**, *46*, 1222–1244.
(10) Gould, P. *Nanotoday* **2006**, *1*, 34–39.
(11) Lin, C. J.; Sperling, R. A.; Li, J. K.; Yang, T.; Li, P.; Zanella, M.; Chang, W. H.; Parak, W. *Small* **2008**, *3*, 334–341.
(12) Gerion, D.; Pinaud, F.; Williams, S. C.; Parak, W. J.; Zanchet, D.; Weiss, S.; Alivisatos, A. P. *J. Phys. Chem. B* **2001**, *105*, 8861–8871.
(13) Yu, W. W.; Chang, E.; Falkner, J. C.; Zhang, J.; Al-Somali, A. M.; Sayes, C. M.; Johns, J.; Drezek, R.; Colvin, V. *J. Am. Chem. Soc.* **2007**, *129*, 2871–2879.
(14) Lewin, M.; Carlesso, N.; Tung, C.; Tang, X.; Cory, D.; Scadden, D. T.; Weissleder, R. *Nat. Biotechnol.* **2000**, *18*, 410–414.
(15) Husseman, M.; Malmstrom, E. E.; McNamara, M.; Mate, M.; Mecerreyes, D.; Benoit, D. G.; Hedrick, J. L.; Mansky, P.; Huang, E.; Russell, T. P.; Hawker, C. J. *Macromolecules* **1999**, *32*, 1424–1431.
(16) Pyun, J.; Matyjaszewski, K. *Chem. Mater.* **2001**, *13*, 3436–3448.
(17) Broyer, R. M.; Quaker, G. M.; Maynard, H. D. *J. Am. Chem. Soc.* **2008**, *130*, 1041–1047.

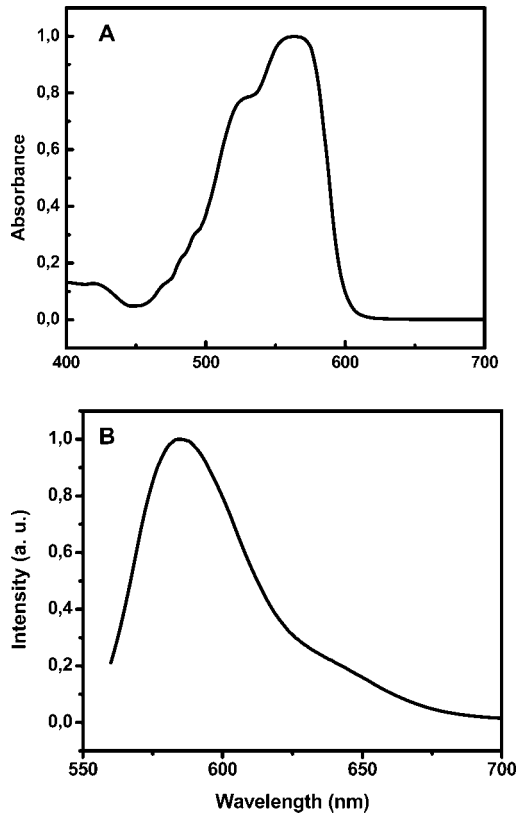

Figure 3. Absorption (A) and photoluminescence spectra (B) of aqueous suspension of Fe_3O_4@MEO_2MA_{90}-*co*-$OEGMA_{10}$-R NPs.

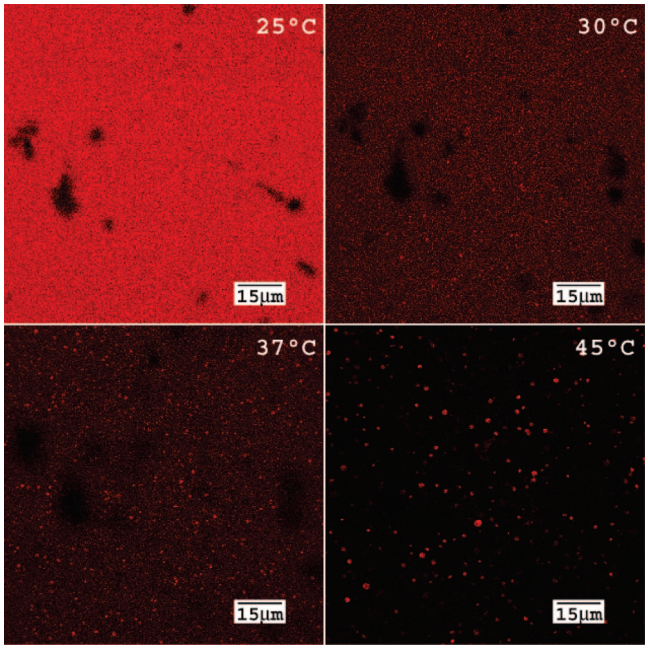

Figure 4. Confocal fluorescence microscopy images of Fe_3O_4@MEO_2MA_{90}-*co*-$OEGMA_{10}$-R NPs in PBS buffer (LCST = 36 °C) when the temperature of the surrounding media increased from 25 to 45 °C.

the NPs in water/oil biphasic systems.[18−20] Stimuli-induced flocculation of stimuli-responsive polymer coated NPs has been studied mainly in organic media.[21] Up to date little effort is devoted to study of flocculation of NPs in aqueous media in response to an environmental stimulus.[19,22] However, one should be aware that the results associated with stimuli-response flocculation of NPs (e.g., transmittance variation versus temperature) may be to some extent misinterpreted as a result of coexistence of free polymer chains in the suspensions. In the present work, we fabricated aqueous, colloidally stable, and thermosensitive Fe_3O_4 NPs by growth of MEO_2MA_x-*co*-$OEGMA_y$ on their surfaces, marked as Fe_3O_4@MEO_2MA_x-*co*-$OEGMA_y$ NPs here, by ligand exchange and studied their agglomeration behavior in physiological media in response to the environmental temperature with the intent of developing the potential biological use. Besides, we also demonstrated the agglomeration reversibility of Fe_3O_4@MEO_2MA_x-*co*-$OEGMA_y$ NPs inside erythrocytes, red blood cells (RBCs), to testify both the biocompatibility of the NPs and the generality of their thermosensitivity in biological media.

Experimental Section

Preparation of Fe_3O_4@MEO_2MA_x-*co*-$OEGMA_y$ NPs. *Materials.* Dopamine hydrochloride (Alfa Aesar), 2-bromoisobutryl bromide (Aldrich), Rhodamine B (Aldrich), 4-vinylbenzyl chloride (Fluka), trimethylsilyl chloride (Alfa Aesar), methacryloyl chloride (Alfa Aesar), 5-aminofluorescein (Fluka), 2-(2-methoxyethoxy) ethyl methacrylate (MEO_2MA, Aldrich), poly(ethylenglyco)-methylether-methacrylat (OEGMA, 475 g/mol, Aldrich), methacryloxyethyl thiocarbamoyl rhodamine B (Polysciences Inc.), and 4,4′-dinonyl-2,2′-dipyridyl (Aldrich) were used as received. Copper(I) bromide (Aldrich) was washed with glacial acid and then with ethanol, filtered, and dried.

Synthesis of Catechol-Functionalized ATRP Initiator, 2-Bromo-N-[2-(3,4-dihydroxy-phenyl)-ethyl]-isobutrylamide. To strongly cap Fe_3O_4 NPs, catechol-terminated initiator was synthesized following the method reported by Messsersmith et al.[23] Typically, a 250 mL round-bottomed flask was charged with $Na_2B_4O_7 \cdot 10H_2O$ (3.83 g, 10 mmol) and 100 mL of water, followed by degassing with argon for 30 min. In the mixture solution, dopamine hydrochloride (1.9 g, 10 mmol) was added. The reaction mixture was stirred for 15 min, and the pH was adjusted to pH 9−10 with $Na_2CO_3 \cdot H_2O$ (3.99 g, 32 mmol). The resulting solution was cooled in an ice bath, and 2-bromoisobutryl bromide (1.24 mL, 2.9 g, 10 mmol) was added dropwise via a syringe. The reaction mixture was allowed to reach room temperature and stirred for 24 h under argon. The pH of the solution was maintained at 9−10 with $Na_2CO_3 \cdot H_2O$ during the reaction. The reaction solution was then acidified to pH = 2 with aqueous HCl solution (6 M) and extracted with acetone ethyl acetate (3 × 100 mL). The combined organic extracts were dried over $MgSO_4$, and the solvent was evaporated under reduced pressure to give a brown liquid. The crude product was purified by silica gel column chromatography (4% methanol in chloroform) to give colorless viscous liquid that was further purified by crystallization from methanol/H_2O to yield white crystals (0.96 g, 3.3 mmol, yield 33%) consisting of the racemic mixture of two enantiomers.

Synthesis of Rhodamine-Labeled Monomers, Tetraethylrhodamine 4-Vinylbenzyl Ester. Tetraethylrhodamine 4-vinylbenzyl ester was synthesized according to the procedures reported by Lutz et al.[24] 4-Vinylbenzyl chloride, rhodamine B, potassium carbonate, and

(18) Duan, H.; Kuang, M.; Wang, D.; Kurth, D.; Möhwald, H. *Angew. Chem., Int. Ed.* **2005**, *44*, 1717–1724.
(19) Edwards, E. W.; Chanana, M.; Wang, D.; Möhwald, H. *Angew. Chem., Int. Ed.* **2008**, *47*, 320–323.
(20) Li, D.; Dunlap, J. R.; Zhao, B. *Langmuir* **2008**, *24*, 5911–5918.
(21) Gelbrich, T.; Feyen, M.; Schmidt, A. M. *Macromolecules* **2006**, *39*, 3469–3472.

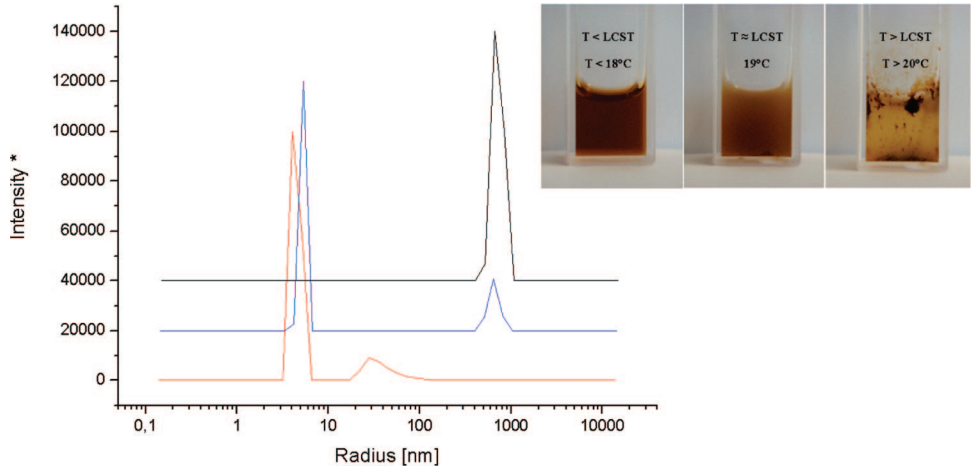

Figure 5. Hydrodynamic size profile of Fe_3O_4@MEO_2MA NPs in PBS at different temperatures: 15 °C (red curve), 19 °C (blue curve), and 21 °C (black curve). The corresponding optical photos are shown in the inset. The LCST of Fe_3O_4@MEO_2MA NPs is 24 °C in water and 20 °C in PBS buffer.

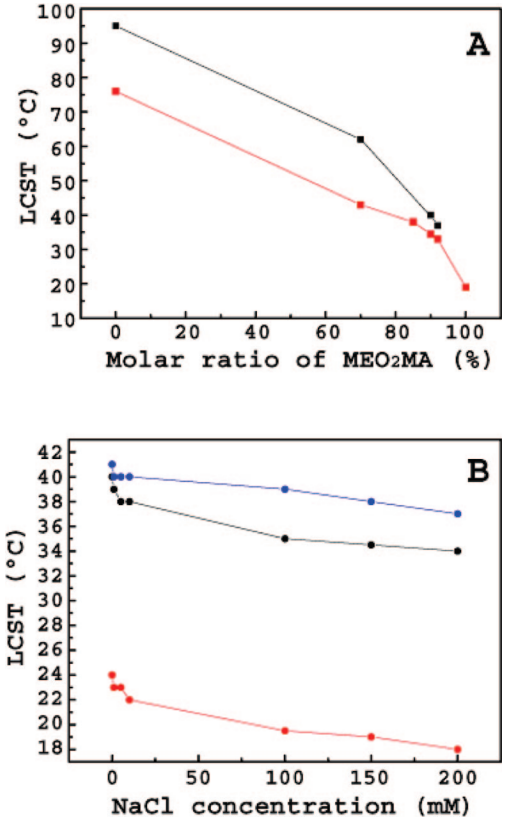

Figure 6. LCST of Fe_3O_4@MEO_2MA_x-*co*-$OEGMA_y$-R NPs versus the molar ratio of MEO_2MA of the polymer capping in water (black) and 150 mM NaCl solution (red). (D) LCST of Fe_3O_4@MEO_2MA_x-*co*-$OEGMA_y$ NPs versus the concentration of NaCl in their suspensions. The molar ratio of MEO_2MA of the polymer capping is 85 (blue), 90 (black), and 100 (red).

DMF were added to a dry three-necked flask. The mixture was stirred for 72 h at 70 °C under argon. After reaction, the solvent was distilled off, and the raw product was purified by column chromatography (9:1 chloroform/methanol, v/v). Both absorption and fluorescence spectra of tetraethylrhodamine 4-vinylbenzyl ester exhibited a slight red shift of roughly 10 nm, as compared to those of rhodamine B. ^{1}H NMR (400 MHz, DMSO-d_6): δ 1.21 (t, 12H), 3,63 (q, 8H), 4,94 (s, 2H), 5,3 (d, 1H), 5,82 (d, 1H), 6,70 (dd, 1H), 6,83 (m, 2H), 6,90 (m, 2H), 6,96 (m, 2H), 7,03 (m, 1H), 7,05 (m, 1H), 7,27 (d, 2H), 7,47 (d, 1H), 7.82−7.92 (m, 2H), 8.27 (d, 1H).

Synthesis of MEO_2MA_x-co-$OEGMA_y$ Polymers. A 100 mL round-bottomed flask was charged with 1 mmol of 4,4′-dinonyl-2,2′-dipyridyl, 0.5 mmol of catechol-functionalized ATRP initiator, 100 mmol of monomers, and 20 mL of toluene. The mixture was degassed with argon for 30 min and 0.5 mmol copper(I)bromide was added. The reaction solution turned light brown. The solution was bubbled for a further 10 min, sealed carefully, and heated to 60 °C. The solution turns dark brown. The polymerization is conducted for 8 h.

To synthesize MEO_2MA_{90}-*co*-$OEGMA_{10}$, for instance, a 100 mL round-bottomed flask was charged with 408.78 mg (1 mmol) of 4,4′-dinonyl-2,2′-dipyridyl, 288.14 mg (0.5 mmol) of 2-bromo-*N*-[2-(3,4-dihydroxy-phenyl)-ethyl]-isobutrylamide, 4.4 mL (10 mmol) of OEGMA, 16.61 mL of MEO_2MA, and 20 mL of toluene. The mixture was degassed with argon for 30 min, and 0.5 mmol copper(I)bromide was added. The solution was bubbled for a further 10 min, sealed carefully, and heated to 60 °C for 8 h.

To synthesize MEO_2MA_{90}-*co*-$OEGMA_{10}$-R, typically, a 100 mL round-bottomed flask was charged with 408.78 mg (1 mmol) of 4,4′-dinonyl-2,2′-dipyridyl, 288.14 mg (0.5 mmol) of 2-bromo-*N*-[2-(3,4-dihydroxy-phenyl)-ethyl]-isobutrylamide, 4.4 mL (10 mmol) of OEGMA, 16.61 mL of MEO_2MA, 2.5 mmol of vinylbenzyl-rhodamine B (1.49 g), and 20 mL of toluene. The mixture was degassed with argon for 30 min, and 0.5 mmol copper (I) bromide was added. The solution was bubbled for further 10 min, sealed carefully, and heated to 60 °C for 8 h.

Synthesis of Fe_3O_4@MEO_2MA_x-co-$OEGMA_y$ NPs. Fe_3O_4@oleate NPs were first synthesized according to the recipe reported by Sun et al.[25] Subsequently, 200 mg of the resulting polymers, either MEO_2MA_x-*co*-$OEGMA_y$ or MEO_2MA_x-*co*-$OEGMA_y$-R, was dissolved in 3 mL of chloroform and mixed with 1 mL of a freshly prepared chloroform suspension of Fe_3O_4@oleate (10 mg/mL). The mixture was stirred at room temperature over 48 h. The polymer coated Fe_3O_4 nanoparticles were precipitated and washed with hexane. After drying, the particles could be dissolved in ethanol. For transferring the NPs into water or salty water, such as PBS buffer, and removal of excess polymer, they were dialyzed against water or buffer for 7 days. To get high particle concentrations, the

(22) Zhu, M.; Wang, L.; Exarhos, G. J.; Li, A. D. Q. *J. Am. Chem. Soc.* **2004**, *126*, 2656–2657.
(23) Fan, X.; Lin, L.; Dalsin, J. L.; Messersmith, P. B. *J. Am. Chem. Soc.* **2005**, *127*, 15843–15847.
(24) Lutz, J.-F.; Pfeifer, S.; Chanana, M.; Thunemann, A. F.; Bienert, R. *Langmuir* **2006**, *22*, 7411–7415.
(25) Sun, S.; Zeng, H.; Robinson, D. B.; Raoux, S.; Rice, P. M.; Wang, S. X.; Li, G. *J. Am. Chem. Soc.* **2004**, *126*, 273–279.

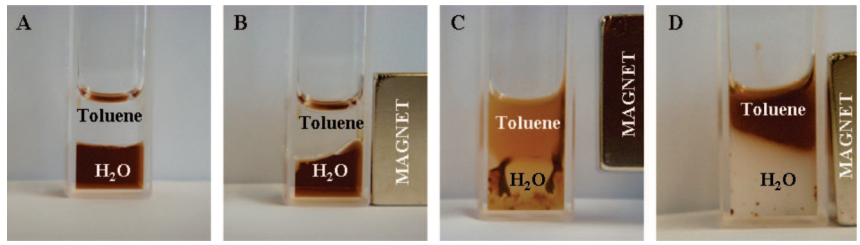

Figure 7. Thermosensitive agglomeration assisted phase transfer of Fe_3O_4@MEO_2MA NPs from PBS buffer phase to toluene phase. The LCST of Fe_3O_4@MEO_2MA NPs is 24 °C in water and 20 °C in PBS buffer. (A) Optical photograph of Fe_3O_4@MEO_2MA NPs in a PBS buffer/toluene biphasic system at 4 °C. The NP concentration is 30 mg/mL. This NP dispersion shows response to a magnet at 4 °C (B). At the temperature of 40 °C, the NPs agglomerated into clumps that were attracted to contact with the toluene phase by a magnet and redispersed into toluene, thus forming homogeneous toluene suspensions (C and D).

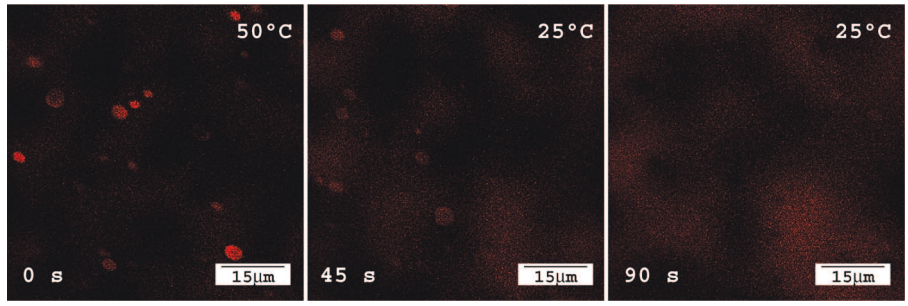

Figure 8. Confocal fluorescence microscopy images of Fe_3O_4@MEO_2MA_{90}-*co*-$OEGMA_{10}$-R NPs in PBS buffer (LCST = 36 °C) when the temperature of the surrounding media decreased from 50 to 25 °C.

particles were precipitated by heating and were collected with a permanent magnet. Then they were redispersed in water or salty water with concentrations of 10−100 mg/mL as required. The resulting Fe_3O_4@MEO_2MA_x-*co*-$OEGMA_y$ NPs were stored at 4 °C.

Characterization. The sizes of Fe_3O_4@MEO_2MA_x-*co*-$OEGMA_y$ NPs were studied by dynamic light scattering (DLS) and transmission electron microscopy (TEM). DLS was performed on a Malvern HPPS 500 and Malvern Zetasizer Nano ZS instrument. TEM images were obtained with a Zeiss EM 912 Omega microscope at an acceleration voltage of 120 kV. The weight fraction of MEO_2MA_x-*co*-$OEGMA_y$ of the resulting NPs was analyzed by TGA. Thermogravimetric analysis (TGA) measurements were performed on NETZSCH TG 209 F1 in aluminum oxide crucible under N_2 atomsphere, in a temperature range of 20−1000 °C, with a heating rate of 10 °C/min.

Study of Thermo-Sensitive Agglomeration Behavior of Fe_3O_4@MEO_2MA_x-*co*-$OEGMA_y$ NPs in Aqueous Media. *DLS.* The thermo-sensitive agglomeration behavior of the resulting Fe_3O_4@MEO_2MA_x-*co*-$OEGMA_y$ NPs was quantitatively studied with the aid of DLS. The particles were dispersed in water or NaCl aqueous solution with different concentrations. The particle concentration was varied from 0.1 mg/mL to 0.5 mg/mL. The size of the particles was measured as a function of the environmental temperature. The temperature range was chosen according to the LCST of the polymers, starting from the temperature 10 °C lower than the LCST. The temperature increment was set as 1 °C, and the incubation time was 1 min. DLS data were obtained by accumulating 3 × 10 measurements of each 10 s. The LCST of Fe_3O_4@MEO_2MA_x-*co*-$OEGMA_y$ NPs was determined by extrapolating the slope toward the *x*-axis and taking the point of intersection (Figure S1, Supporting Information).

Confocal Laser Scanning Microscopy (CLSM). The thermo-sensitive agglomeration behavior of the resulting Fe_3O_4@MEO_2MA_x-*co*-$OEGMA_y$-R NPs was qualitatively visualized by CLSM, which was performed on a Leica SP5 Confocal Microscope. In the case of Fe_3O_4@MEO_2MA_{90}-*co*-$OEGMA_{10}$-R with a LCST of 43 °C in water and 36 °C in salty water, the NPs were placed in a temperature controlled chamber for CLSM observation, and the temperature was increased with 2 °C/min via a water circulation bath from 25 °C until 60 °C. Then, the water bath was cooled back to 25 °C by adding ice into the bath. The particles were well dispersed at 25 °C, leading to a homogeneous bright fluorescence. With increasing temperature the NPs slowly started agglomeration, the fluorescence became weaker, and at 41 °C they agglomerated into clumps with an average size of approximately 2 μm. By cooling the sample back to 25 °C, the NP clumps first swelled up to approximately 5 μm and dis-agglomerated into isolated NPs again. At this point no aggregates are visible anymore.

Study of Thermo-Sensitive Agglomeration Behavior of Fe_3O_4@MEO_2MA_x-*co*-$OEGMA_y$-R NPs inside RBCs. *Isolation of Human RBCs.* Blood was withdrawn from healthy volunteers by venous puncture and anticoagulated using ethylene diamine tetraacetic acid. Following anticoagulation, blood samples were processed immediately. Packed RBCs with a hematocrit of 80% were obtained by removing plasma and buffy coat through centrifugation and three washing steps with phosphate buffered saline (PBS, pH 7.4, 300 mOsm) at 2000 rpm.

Loading of Fe_3O_4@MEO_2MA_x-co-$OEGMA_y$-R NPs into RBCs. The encapsulation of nanoparticles into the RBCs was accomplished by hypo-osmotic dilution. For this purpose, 1 mL of packed RBCs was subjected to 50 to 200 μL aqueous suspensions of the NPs, in either PBS or H_2O. Immediately after that, H_2O was added in a quantity to reach a final osmolarity of 80 mOsm. Under these conditions resealable pores within the RBC membrane of a size between 200 and 500 Å in diameter were created. FITC−bovine serum albumin (BSA) together with the NPs were incorporated simultaneously into the RBCs. After adding the hypo-osmotic solutions and the substances to be encapsulated, the sample was mixed 15 times by inversion, incubated for 1 h under stirring conditions and dialyzed against 25% poly(ethylene glycol) in PBS (pH 8) for another hour using a 3.5 kDa dialysis filter (Mini Dialysis Units, Pierce, U.S.A.), both at 4 °C. Thereafter, 150 μL of a hyper-osmotic buffer consisting of 5 mM adenine, 100 mM inosine, 100 mM sodium pyruvate, 100 mM glucose, and 12% (w/v) sodium

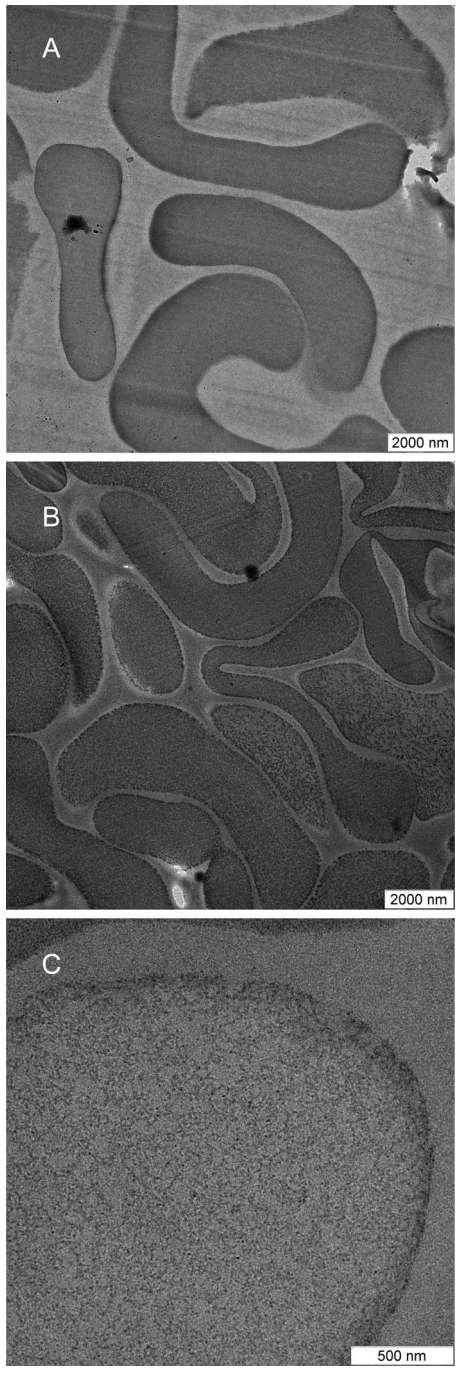

Figure 9. TEM image of the ultrathin sections of RBCs loaded without (A) and with Fe_3O_4@OEGMA (B). (C) High magnification TEM images of the ultrathin sections of RBCs loaded with Fe_3O_4@OEGMA.

chloride while incubating for 1 h at 37 °C was rapidly added to anneal and reseal the opened RBCs. To remove unentrapped NPs, hemoglobin, and cell constituents, the NP-loaded RBCs were washed three times with isotonic PBS for 15 min at 320 g. The supernatant was discarded. Each preparation included a control sample, which was exposed to the loading procedure without incorporating nanoparticles or bioactive substances.

Study of Thermo-Sensitive Agglomeration Behavior of RBCs Loaded with Fe_3O_4@MEO_2MA_x-co-$OEGMA_y$-R NPs by Means of CLSM. The NP-loaded RBCs in PBS buffer were placed in the temperature controlled chamber for CLSM, and the temperature was increased with 2 °C/min via a water circulation bath from 25 °C until 40 °C. In the case of Fe_3O_4@MEO_2MA_{90}-*co*-$OEGMA_{10}$-R NPs, for instance, the particles in the RBCs were well dispersed at 25 °C, start agglomeration, and completely agglomerated into clumps at 37 °C. Then, the water bath was cooled back to 25 °C by adding ice into the bath. The NP aggregates in the RBCs redispersed again, and the homogeneous fluorescence was recovered inside the RBCs. BSA-FITC was loaded in RBCs together with NPs as a control substance for the aggregation behavior. In the case of Fe_3O_4@MEO_2MA-R NPs with a LCST of 24 °C in water and 20 °C in salty water, the temperature range was set from 4 °C to room temperature (25 °C).

Magnetic Resonance Imaging (MRI). MRI was performed using a 7 T rodent scanner (Pharmascan 70/16AS, Bruker BioSpin, Ettlingen, Germany) with a 16 cm horizontal bore magnet and a 9 cm (inner diameter) shielded gradient with a H-resonance frequency of 300 MHz and a maximum gradient strength of 300 mT/m. For imaging, a ^{1}H-RF volume resonator with an inner diameter of 38 mm was used. Data acquisition and image processing were carried out by means of the Bruker software Paravision 4.0. T2- and T1-weighted 2D turbo spin−echo sequences were used (imaging parameters: for T1 TR/TE = 900/10 ms, RARE factor 2, 4 averages, and for T2 TR/TE = 3500/36 ms, RARE factor 8, 4 averages) to image the temperature dependent behavior of the nanoparticles within the RBCs. A field of view (FOV) of 3 cm^2, matrix 128 × 128, and a slice thickness of 1 mm represent further setting parameters. To calculate the T2 relaxation time, a T2 weighted multislice multiecho sequence with 16 echoes was applied (MSME-T2fit, TR 1000 ms, TE 8.6−138 ms).

Results and Discussion

MEO_2MA_x-*co*-$OEGMA_y$, as a new class of thermosensitive polymers, is of compelling interest for biomedical use as a result of their excellent biological compatibility arising from their oligo(ethylene glycol) side groups.[26] It shows a lower critical solution temperature (LCST) in water. Such copolymers have demonstrated the possibility to tune the surface energy of gold NPs to transfer the NPs across the salty water/oil interface.[19] To cap Fe_3O_4 NPs we synthesized a new ATRP initiator from dopamine, 2-bromo-*N*-[2-(3,4-dihydroxy-phenyl)-ethyl]-propionamide, whose catechol group can be strongly coupled with the surface of iron oxide particles.[23] This new initiator was used to synthesize MEO_2MA_x-*co*-$OEGMA_y$ with different molar ratio of MEO_2MA to OEGMA, listed in Table 1. MEO_2MA_x-*co*-$OEGMA_y$ was fluorescently labeled by copolymerization with vinylbenzyl-rhodamine (2 mol %), marked as MEO_2MA_x-*co*-$OEGMA_y$-R (R = rhodamine). The 6−9 nm Fe_3O_4 NPs were synthesized in chloroform via pyrolysis of ferric acetylacetonate in the presence of oleic acid and oleylamine.[25] MEO_2MA_x-*co*-$OEGMA_y$ was capped on Fe_3O_4 NPs via ligand exchange in chloroform (Figure 1). As analyzed by DLS and TEM, the polymer coated NPs were 15−25 nm in size and the polymer shells were 5−8 nm in thickness (Table 1 and Figure 2). Furthermore, the coating of MEO_2MA_x-*co*-$OEGMA_y$-R rendered the NPs photoluminescent (Figure 3).

As a result of the presence of oligo(ethylene glycol) side groups on the surfaces, Fe_3O_4@MEO_2MA_x-*co*-$OEGMA_y$ NPs can be dispersed in water and exhibit a robust colloidal stability against salt, being stable for months in PBS buffer or 150 mM NaCl aqueous solutions without detectable agglomeration. Thermogravimetric analysis suggested a

(26) Lutz, J.-F. *J. Poly. Sci., Part A: Polym. Chem.* **2008**, *46*, 3459–3470.

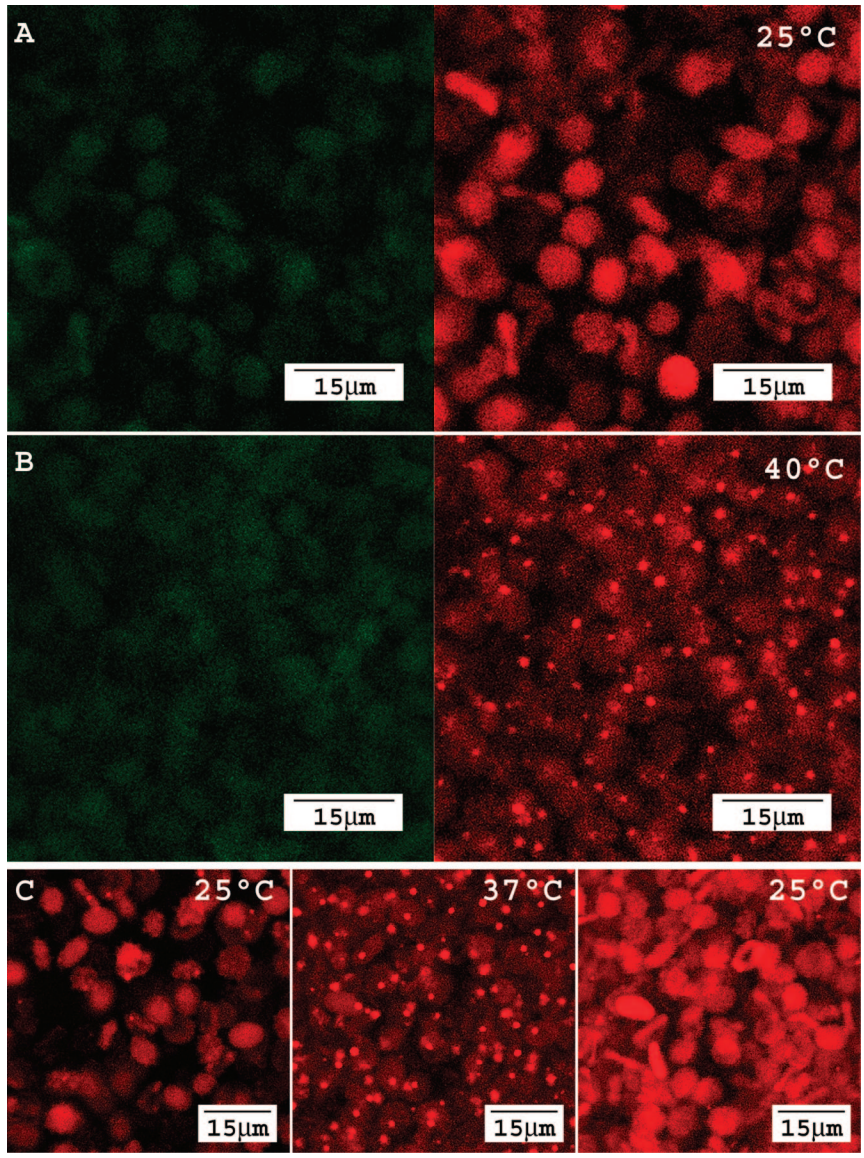

Figure 10. (A and B) Confocal fluorescence microscopy images of RBCs loaded with both Fe_3O_4@MEO_2MA_{90}-*co*-$OEGMA_{10}$-R NPs (LCST = 36 °C in PBS) and FITC−bovine serum albumin labeling the inner volume of RBCs at 25 °C (A) and 40 °C (B). Note that FITC−bovine serum albumin was used as the control to label RBCs. The left panel was recorded using the FITC channel and the right using the rhodamine one. (C) Confocal fluorescence microscopy images of RBCs loaded with both Fe_3O_4@MEO_2MA_{90}-*co*-$OEGMA_{10}$-R NPs and FITC−BSA when the environmental temperature first increased from 25 to 37 °C and then decreased back to 25 °C.

moderate grafting density of MEO_2MA_x-*co*-$OEGMA_y$ on the NPs around 150−200 chains per NP. As such one can expect that the MEO_2MA_x-*co*-$OEGMA_y$ brushes capped on Fe_3O_4 NPs behave similarly as they do in solution.[27]

As shown in Figure 4 and Movie S1 (Supporting Information), when the surrounding temperature increased above a critical point, Fe_3O_4@MEO_2MA_x-*co*-$OEGMA_y$ NPs started to agglomerate into more than 2 μm aggregates in 30 s. As analyzed by DLS, over a larger temperature range around this critical temperature, a bimodal size distribution was observed in aqueous suspensions of the Fe_3O_4@MEO_2MA_x-*co*-$OEGMA_y$ NPs, suggesting the coexistence of isolated NPs and NP aggregates (Figure 5). The critical temperatures for Fe_3O_4@MEO_2MA_x-*co*-$OEGMA_y$ NPs to start agglomeration were comparable to the LCSTs of the MEO_2MA_x-*co*-$OEGMA_y$ used to coat the NPs, which were determined by DLS and referred to as the NP LCSTs listed in Table 1. The aggregates were not stable and eventually precipitated from aqueous media with temperature (Figure S2, Supporting Information). Similar to that of free MEO_2MA_x-*co*-$OEGMA_y$ chains in solution[26] and those grafted on planar substrates,[27] the LCST of Fe_3O_4@MEO_2MA_x-*co*-$OEGMA_y$ NPs decreased with MEO_2MA molar fraction (Figure 6A). Besides, the NP LCST also decreased with salt concentration (Figure 6B), as a result of the salting-out effect on the hydrogen bonding between the polymer grafted on the NPs and the surrounding water.[26]

Furthermore, when the surrounding temperature was above the LCST of Fe_3O_4@MEO_2MA_x-*co*-$OEGMA_y$ NPs, the aggregates were easily collected by a magnet (Figure S2, Supporting Information). By pulling in contact with toluene with a magnet, the aggregates can be redispersed into toluene (Figure 7), indicating the hydrophobic surface character of Fe_3O_4@MEO_2MA_x-*co*-$OEGMA_y$ NPs above the LCST. At

(27) Jonas, A. M.; Glinel, K.; Oren, R.; Nysten, B.; Huck, W. T. S. *Macromolecules* **2007**, *40*, 4403–4405.

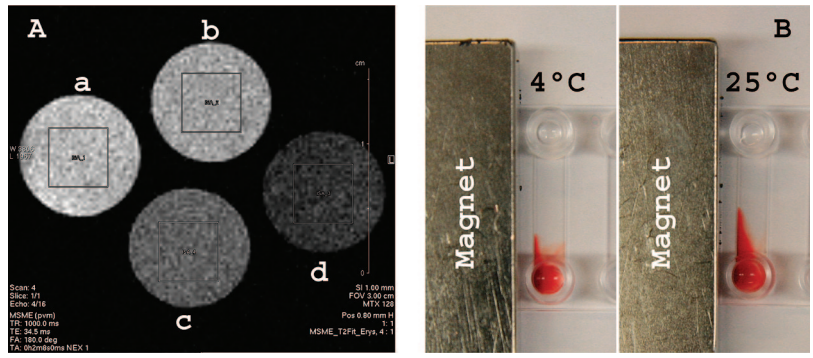

Figure 11. (A) MRI images of phantom tubes containing 1×10^5 RBCs (a and b) and those loaded with Fe_3O_4@MEO_2MA NPs (LCST = 20 °C) (c and d). Tubes a and c were fixed at 4 °C and tubes b and d at 37 °C. The four slices were simultaneously placed into the magnet so the gray scales can be compared. (B) Photographs of using a magnet to manipulate RBCs loaded with Fe_3O_4@MEO_2MA NPs at 4 °C (left panel) and 25 °C (right panel).

the suggestion of our previous report, this dual dispersibility should be characteristic for NPs coated with stimuli-responsive polymers.[18,19] This is also the main reason for NP agglomeration.[19]

Most peculiarly, cooling leads to disagglomeration. Isolated Fe_3O_4@MEO_2MA_x-*co*-$OEGMA_y$ NPs reappeared when the surrounding temperature was below the LCST (Figure 8 and Movie S2, Supporting Information). This reverse agglomeration can be repeated for tens of times, and the long time storage had little influence on the agglomeration reversibility of the NPs. The reason for the complete disagglomeration is expected to be twofold. First, the polymer coating may reduce the van der Waals and magnetic dipolar attraction of the Fe_3O_4 cores, enabling redispersion. Second, oligo(ethylene glycol) grafted polymers are expected to have the excellent steric repulsion. Taken together, this demonstrates the reversibility of this temperature-induced agglomeration.

Thanks to their morphology and flexibility,[27] erythrocytes (RBCs) have been extensively investigated as potential biocompatible carriers for different bioactive substances including peptides and enzymes.[28−30] Having the advantage of being biodegradable and nonimmunogenic, RBCs can carry large volumes of entrapped drugs per unit volume of cells. To explore the potential of using the thermo-sensitive and reversible agglomeration of Fe_3O_4@MEO_2MA_x-*co*-$OEGMA_y$ NPs in biomedical applications, they were loaded into RBCs via hypo-osmotic dilution.[31] The presence of the oligo(ethylene glycol) side groups rendered Fe_3O_4@MEO_2MA_x-*co*-$OEGMA_y$ NPs stable against hemoglobin adsorption and, at the same time, noncytotoxic (the data are not shown here), similar to the study of Fe_3O_4@ OEGMA.[32] Thus, we succeeded in loading 1−10 mg/mL NPs into one RBC. TEM imaging of the ultrathin sections of the NP-loaded RBCS clearly showed the NPs were exclusively located inside the RBCS (Figure 9). Figure 10A shows the homogeneous distribution of fluorescent Fe_3O_4@MEO_2MA_x-*co*-$OEGMA_y$-R inside the RBCs. When the surrounding temperature was increased close to or slightly above the LCST, the NPs agglomerated inside RBCs (Figure 10B and Movie S3, Supporting Information). Like they were in aqueous media, the NP aggregates in RBCs could also be disagglomerated into isolated NPs by cooling (Figure 10C and Movie S4, Supporting Information). This reverse agglomeration of the NPs inside the RBCs can be repeated for at least five times (within the time scale of the RBC lifetime).

Fe_3O_4 NPs can predominantly reduce the transverse relaxation, that is, T2 decay of the surrounding water protons under a steric magnetic field, leading to a negative contrast of mainly T2-weighted MRI.[8] Figure 11A shows the T2-weighted MRI pictures of RBCs loaded with Fe_3O_4@MEO_2MA_x-*co*-$OEGMA_y$ NPs. When the surrounding temperature increased above the NPs' LCST, the signal intensity in T2 imaging decreased considerably by 44% as compared to that obtained at the temperature below the LCST, and the T2 relaxation time was reduced from 25 ms to 20 ms. In contrast, such heat treatment caused an intensity decrease of 9% in T2 imaging of pure RBCs. Figure 11B shows that upon the increase of the surrounding temperature, agglomeration aids a stronger attraction of NP-loaded RBCs to a magnet. Taken together, this demonstrates that one can largely improve the magnetic retention of Fe_3O_4@MEO_2MA_x-*co*-$OEGMA_y$ NPs loaded in RBCs by increasing the surrounding temperature to induce agglomeration of the NPs.

Conclusion

We have synthesized catechol-terminated MEO_2MA-*co*-OEGMA copolymers with varied ratios of MEO_2MA to OEGMA using catechol-functionalized ATRP initiators via ATRP. The resulting polymers have been grafted on organic Fe_3O_4 NPs via ligand exchange, leaving behind aqueous and colloidally stable Fe_3O_4@MEO_2MA_x-*co*-$OEGMA_y$ NPs. Copolymerization of MEO_2MA and OEGMA with dye-labeled monomers allows formation of fluorescent polymer coating on Fe_3O_4 NPs, leading to both fluorescent and magnetic NPs. Of paramount importance is that the resulting composite NPs exhibit a thermosensitivity; the NP LCST is comparable to that of the polymer brushes coated on the NPs. Thanks to this thermosensitivity and the strong steric repulsive interaction between the polymer coatings on their surfaces, Fe_3O_4@MEO_2MA_x-*co*-$OEGMA_y$ NPs can reversibly agglomerate in response to the environmental temperature change in buffer and physiological solution. The same reversible thermosen-

(28) Dischер, D. E.; Mohandas, N.; Evans, E. A. *Science* **1994**, *266*, 1032–1305.
(29) DeLoach, J. R. *Med. Res. Rev.* **1986**, *6*, 487–504.
(30) Kinosita, K. Jr.; Tsong, T. Y. *Nature (London)* **1978**, *272*, 258–260.
(31) Brähler, M.; Georgieva, R.; Buske, N.; Müller, A.; Müller, S.; Pinkernelle, J.; Teichgräber, U.; Voigt, A.; Bäumler, H. *Nano Lett.* **2006**, *6*, 2505–2509.
(32) Lee, H.; Lee, E.; Kim, D. K.; Jang, N. K.; Jeong, Y. Y.; Jon, S. *J. Am. Chem. Soc.* **2006**, *128*, 7393–7389.

sitive agglomeration has been also achieved inside RBCs. The agglomeration of Fe_3O_4@MEO_2MA_x-*co*-$OEGMA_y$ NPs can significantly enhance the magnetic response of the loaded RBCs as a whole, thus dramatically enhancing the MRI contrast and allowing manipulation of the RBCs with an external magnet.

As a result of the excellent reversibility and many variants of local heat treatment, for instance, by light or microwaves, thermosensitive agglomeration of Fe_3O_4@MEO_2MA_x-*co*-$OEGMA_y$ NPs allows control of not only the intensity but also the location of the NPs' magnetism and thus leads to innovative biomedical uses. We demonstrate here MRI and magnetic manipulation. On the other hand, reversibly tuning agglomeration of NPs creates a dynamic equilibrium between agglomeration and disagglomeration, thus leading to dynamic self-organization of NPs in response to environmental stimuli. This should provide a temporal control over the spatial organization of NPs and lead to unprecedented material properties. Hence, the procedure demonstrated here will be applicable not only on magnetic but also on other NPs with different collective optical and electrical properties, opening ways toward new applications in materials and biomedical sciences.

Acknowledgment. The project is supported by the Max Planck Society. D.W. is in part supported by a DFG grant (WA1704/4-1) and an EU-STREP grant (BONSAI, LSHB-CT-2006-037639), and R.G. and H.B. are supported by DFG grants (EFRE-ProFIT 10134275 and 10139827). S.J. thanks Cambridge European Trust from the University of Cambridge, U.K., for a research fellowship. R. Knorr is thanked for experimental assistance. The authors are indebted to H. Möhwald for helpful discussion and support.

Supporting Information Available: Plot of hydrodynamic diameters and optical photographs (PDF) and the movies mentioned in the text (MPG). This material is available free of charge via the Internet at http://pubs.acs.org.

CM900126R